



HAL
open science

First detection of the supersonic upward plasma flow structures in the early morning sector

Elvira Astafyeva, Irina Zakharenkova

► **To cite this version:**

Elvira Astafyeva, Irina Zakharenkova. First detection of the supersonic upward plasma flow structures in the early morning sector. *Geophysical Research Letters*, 2015, 142, pp.9642-9649. 10.1002/2015JA021447 . insu-01514041

HAL Id: insu-01514041

<https://insu.hal.science/insu-01514041>

Submitted on 25 Apr 2017

HAL is a multi-disciplinary open access archive for the deposit and dissemination of scientific research documents, whether they are published or not. The documents may come from teaching and research institutions in France or abroad, or from public or private research centers.

L'archive ouverte pluridisciplinaire **HAL**, est destinée au dépôt et à la diffusion de documents scientifiques de niveau recherche, publiés ou non, émanant des établissements d'enseignement et de recherche français ou étrangers, des laboratoires publics ou privés.



RESEARCH LETTER

10.1002/2015GL066369

Key Points:

- First observations of the supersonic upward drift in the early morning sector
- Two supersonic events were detected quasi-simultaneously over the eastern Pacific
- Such events are extremely rare to occur in the early morning sector

Supporting Information:

- Supporting Information S1

Correspondence to:

E. Astafyeva,
astafyeva@ipgp.fr

Citation:

Astafyeva, E., and I. Zakharenkova (2015), First detection of the supersonic upward plasma flow structures in the early morning sector, *Geophys. Res. Lett.*, *42*, 9642–9649, doi:10.1002/2015GL066369.

Received 1 OCT 2015

Accepted 28 OCT 2015

Accepted article online 4 NOV 2015

Published online 23 NOV 2015

First detection of the supersonic upward plasma flow structures in the early morning sector

Elvira Astafyeva¹ and Irina Zakharenkova¹

¹Institut de Physique du Globe de Paris, Paris Sorbonne Cité, Paris VII - Denis Diderot University, UMR CNRS 7154, Paris, France

Abstract We present the first observations of the supersonic updrafting plasma drifts in the predawn sector. Two DMSP satellites quasi-simultaneously detected two fast-speed events: one of ~385 km spatial extension and with the maximum upward velocity of 1683 m/s appeared at ~3 LT, and the other of ~1500 km large with maximum speed of 1770 m/s occurred at ~5 LT. Both supersonic structures were observed above the eastern Pacific region, separated by ~35° of longitude in space and by 45 min in time. The events occurred at the recovery phase of the geomagnetic storm of 19 February 2014, during rapid oscillations of the interplanetary magnetic field B_z and the interplanetary electric field E_y components, which increased the eastward electric field in the equatorial nighttime ionosphere and triggered the generation of plasma irregularities. The storm time penetration electric fields seem to be the principal driver of the observed supersonic events.

1. Introduction

Irregularities in the ionospheric plasma density, also known as ionospheric irregularities, often cause amplitude and phase scintillations of radio waves and, consequently, can seriously disrupt the radio-based communication [e.g., *Basu et al.*, 2008; *Demyanov et al.*, 2012; *Astafyeva et al.*, 2014; *Kelly et al.*, 2014]. Very intensive ionospheric irregularities often occur at equatorial latitudes after sunset (often referred to as equatorial spread-F, ESF). Without solar ionization, the ions recombine and form a lower density layer, which, in turn, is unstable to plasma interchanges. The Rayleigh-Taylor (R-T) instability, along with $E \times B$ instability, is the main cause of generation of large-scale density depletions at the bottom of the F layer, which can further rise as high as 1000 km [Woodman and La Hoz, 1976; Ott, 1978; Fejer et al., 1999; Burke et al., 2003].

Contrary to the postsunset ionospheric irregularities and plasma bubbles that occur quite often after sunset, the postmidnight events are rare to observe [e.g., *Burke et al.*, 2009; *Yokoyama et al.*, 2011; *Huang et al.*, 2013; *Yizengaw et al.*, 2013]. Even more rare events are occurrences of intensive ionospheric irregularities and/or plasma bubbles in the predawn sector. Those were occasionally observed at the recovery phase of magnetic storms [e.g., *Yeh et al.*, 2001; *Li et al.*, 2012; *Zakharenkova and Astafyeva*, 2015; *Zakharenkova et al.*, 2015] or even under geomagnetically quiet and during solar minimum conditions [de la Beaujardière et al., 2009; *Dao et al.*, 2011; *Gentile et al.*, 2011]. The results from Communications/Navigation Outage Forecasting System (C/NOFS) satellite suggested that during geomagnetically quiet conditions, a passage of the solar terminator and the associated upward plasma drifts can serve as a source of such irregularities [de la Beaujardière et al., 2009].

Concerning the dynamical characteristics of the ionospheric irregularities and plasma bubble structures, they are known to drift in the zonal direction, eastward in the postsunset sector and night, westward in the early morning, and the reversal of the zonal drift velocity occurs around 04 LT [Abdu et al., 1985; Fejer et al., 1991; Huang et al., 2010]. Concerning the vertical plasma drift velocities, in the majority of cases, they lie within ± 100 –150 m/s [Woodman and La Hoz, 1976; Hysell et al., 1994; Patra et al., 2005]. Inside plasma bubbles the plasma drift velocity can reach as high as ± 800 m/s but usually varies around ± 300 –400 m/s [Huang et al., 2010].

Aggson et al. [1992] seemed to be the first to report observations of supersonic upward drifting plasma bubbles. By using plasma and electric field observations from San Marco D and Dynamics Explorer 2 (DE 2) satellites, Aggson et al. [1992] observed occurrence of two events of plasma bubbles updrafting at ~1.7–1.9 km/s. Both events were observed at equatorial latitudes and at the postsunset-premidnight sectors, one at ~20.5 LT and the other at ~23.2 LT, at an altitude of 400–500 km. The bubbles were observed to accelerate upwards at ~0.5 g. Following this first time detection, Burke and Aggson [1993] further developed a model for nonlinear supersonic equatorial plasma bubbles and suggested that such high-speed structures can only be detected “if the satellite crosses the bubble wall on field lines that

thread through its upper boundary at the equator." *Hysell et al.* [1994] used the Cornell University 50 MHz portable radar interferometer (CUPRI) and observed ~ 1200 m/s upward plasma drift velocities over Kwajalein. The event was observed at 600–700 km and only lasted for 10 min. *Hanson et al.* [1997] used data from the ion drift meter onboard the Defense Meteorological Satellite Program (DMSP) F9 and F10 spacecraft and revealed that the upward ion drifts exceeding 800 m/s but less than the sound speed can occur as often as in 40% of observations but only just after sunset. The authors suggested that the observed upward plasma acceleration was due to the postsunset enhanced electric field. More recently, *Huba and Joyce* [2007] developed a new two-dimensional code (NRLESF2) to simulate the nonlinear development of plasma bubbles and demonstrated the first ESF simulation results of supersonic flows within low-density channels.

Thus, the supersonic upward plasma drifts were observed occasionally, but all observations seemed to be done in the postsunset-premidnight sectors. In this paper, we report the first observations of supersonic upward drifting large-scale structure in the postmidnight-predawn sector.

2. Data Used

Our main results rely on observations from the DMSP satellites F15, F16, and F17. The DMSP spacecrafts are placed in a near-circular, sun-synchronous, polar orbit with inclination 98.8° – 98.9° (<http://dmsp.ngdc.noaa.gov>). The orbital altitude is ~ 835 – 855 km, and the period is ~ 102 min. During the 19 February 2014 event, the descending equator crossing time for the satellites was F15, 3.06 LT; F16, 4.95 LT; and F17, 5.95 LT.

In this work, we use data from the following instruments on board these satellites: (1) data from the ion drift meter (IDM) to get the vertical (V_z) and zonal cross-track (V_y) ion drift velocities, (2) scintillation meter (SM) to get the total ion density N_i , (3) Langmuir Probe to get the electron temperature (T_e) and electron density (N_e), (4) retarding potential analyzer (RPA) to get the ion temperature (T_i) and plasma composition (O+, H+, and He+), and (5) triaxial fluxgate magnetometer on board DMSP F16 to get the variations of the magnetic field along the satellite pass (these data were not available for the DMSP F15).

3. Results

The storm of 19 February 2014 was rather complex: a coronal mass ejection arrival was detected at $\sim 2:20$ UT on 19 February, but no classical sudden storm commencement was recorded in the ground-based magnetic data as can be seen in the *SYM-H* variations (Figure 1b). By that time, the interplanetary magnetic field (IMF) B_z component already equaled to -8 nT, and from $\sim 4:00$ UT it further intensified down to -15 nT. The IMF B_z remained negative until $\sim 9:10$ UT, when it turned northward for the next 2 h (Figure 1b) and marked the beginning of the recovery phase of the storm. From 12 UT to 13:35 UT the IMF B_z turned southward for the second time. From 13:35 UT it remained positive.

In this paper, we will focus on the period 10.3 UT–11.7 UT (shaded by the light green rectangle in Figure 1), when F15, F16, and F17 DMSP satellites flew over the eastern Pacific region (Figure 2, left). The main plasma parameters as derived by the three DMSP satellites are shown in Figure 3. DMSP F16 flew above the considered region from 10.3 to 10.7 UT and registered a sharp increase in the vertical plasma drift velocity up to 1683 m/s while passing over the area (-3.6° to -7.1° Geographic latitudes (Glat); 275.8° to 275.0° Geographic longitudes (Glon)) at ~ 854.7 km of altitude. The maximum velocity values were registered at 10:32–10:33 UT, which corresponds to 4.79 LT, ~ 6 – 7° of latitude on the north from the magnetic dip equator (Figure 2). Figure 3a shows that within the high-speed plasma flow structure, the horizontal velocity changed sharply from 0 to -750 m/s, and intensive fluctuations in the ion and electron density, as well as in the light ions (O+ and H+, He+), occurred. Within this "turbulent" area, the ion and electron temperatures fluctuated as well (Figure 3a, top panel), and the electric field E_y reached as high as 31 mV/m (Text S1 and Figure S1b in the supporting information). At the same time, the vertical component of the magnetic field fluctuated within ± 15 nT (Figure S1c). These magnetic variations are about 10 times less than those observed by *Aggson et al.* [1992] inside supersonic bubble event at ~ 500 – 600 km of altitude.

In addition to this first fast-speed irregular structure, data of DMSP F16 show another spot with rapid fluctuations of the plasma density and temperature below the magnetic dip equator around the area (-20° to -35° Glat); the

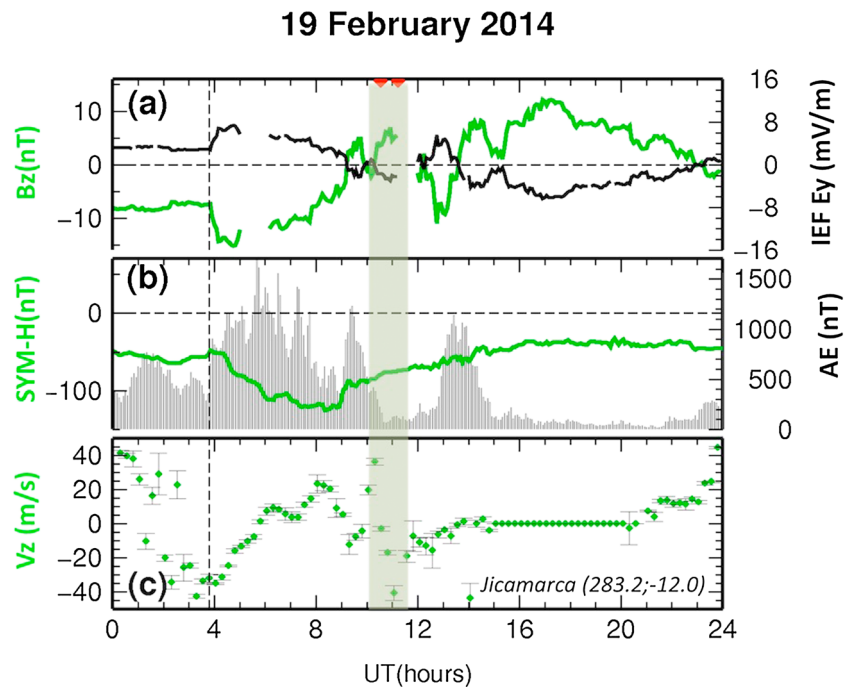


Figure 1. Variations of the interplanetary and geophysical parameters during the 19 February 2014 moderately intense geomagnetic storm. (a) IMF B_z component (green) and IEF E_y component (black); orange triangles show the occurrence time of the two supersonic events; (b) auroral electrojet (AE) index (gray bars) and the SYM-H index (green curve); (c) 5 min averaged variations of the vertical ionospheric drift above the Jicamarca ionosonde station (green diamonds); the error bars are shown in black thin lines.

vertical plasma drift velocities within this second “turbulent” region exceeded the normal values of ± 100 – 150 m/s and reached -500 m/s (Figures 2 and 3a).

DMSP F17 sounded almost the same area as F16 but 1 h later and revealed a significant decrease in the plasma drift velocity (Figures 2, 3a, and 3c). Over the first turbulent area, the signatures of the high-speed plasma motion disappeared during this time. The second spot could still be observed in the data of F17, though the amplitude of the plasma density fluctuations as well as of V_x and V_z values decreased as compared to F16 measurements, while the temperature increased (Figures 3a and 3c).

Our second example of the very fast plasma upflow was observed in data of the DMSP F15 satellite from 11:08 to 11:13 UT, when the satellite crossed the region ($+10^\circ$ to -5° GLat; 237.2 – 237.7° E GLon) (Figures 2 and 3b). This second fast upward flow structure appeared to be more spatially extended than the first one and was detected around the magnetic dip equator (Figure 2). The maximum value of the upward drift of 1770.6 km/s was registered at 11:11:30 UT (corresponds to 03.04 LT). Simultaneously, the horizontal speed also increased from ~ 200 m/s to 1000 – 1200 m/s. Unlike the previous examples, this event was accompanied first by a short-term increase and then by a clear depletion in the electron and ion densities, indicating that the high-speed drift was measured inside a plasma bubble.

It should be pointed out that such high values of upward plasma drift velocities are quite unusual, as they exceed ~ 10 – 15 times the background values of ± 100 – 150 m/s [McClure et al., 1977; Patra et al., 2005]. The observed upflow events could be supersonic if the observed velocities overcome the local sound speed. To estimate the ion sound velocity for O^+ ions for the two observed events, we use the following formula [Huba, 2013]:

$$C_s = \sqrt{\frac{\gamma Z k T_e}{m_i}} = 9.79 \cdot 10^5 \sqrt{\frac{\gamma Z T_e}{\mu}} \quad (1)$$

where k is Boltzmann’s constant, Z is charge state, γ is the adiabatic index, m_i is ion mass, $\mu = m_i/m_p$ is the ion mass expressed in units of the proton mass, and T_e is the electron temperature. Taking $\gamma = 1.667$ and $\mu = 16$, and the real electron temperatures measured by the DMSP during the high-speed events registrations, we

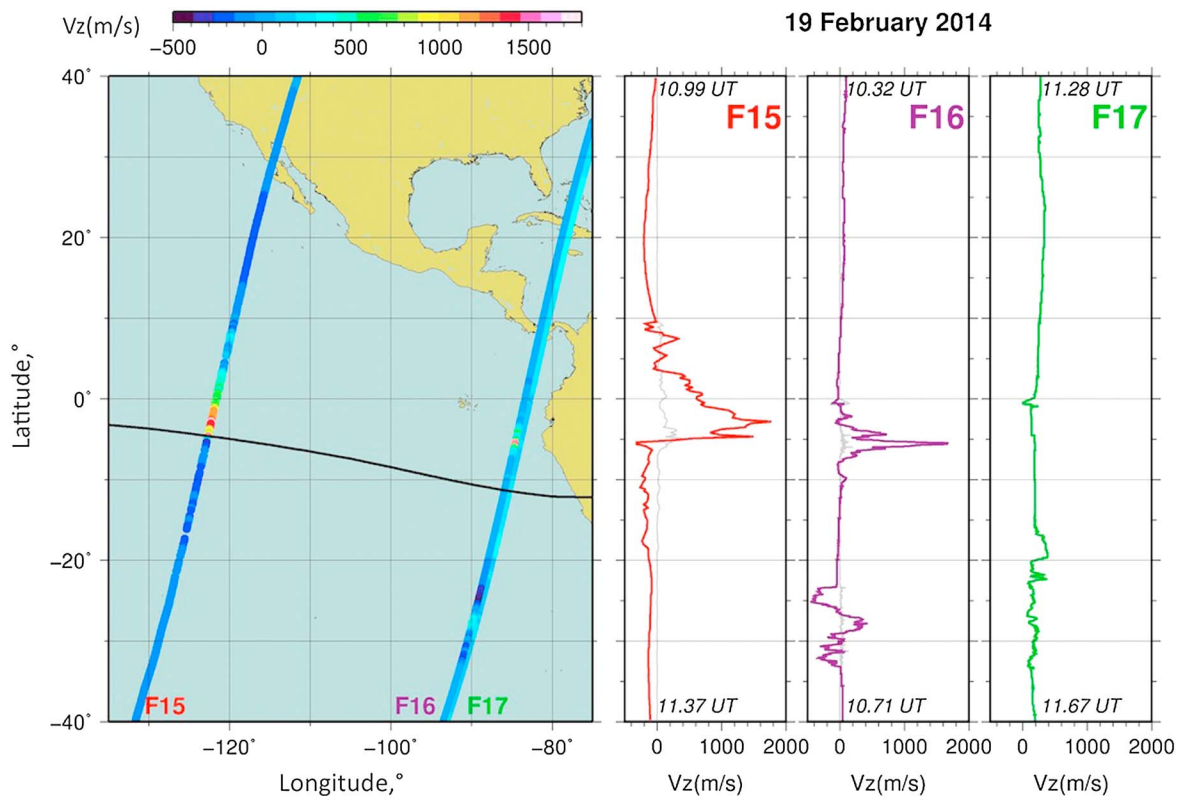


Figure 2. (left) Trajectories of the DMSP F15 (red label), F16 (violet label), and F17 (green label) satellite passes during ~10.3–11.7 UT on 19 February 2014. The color codes along the passes show the value of the upward drift velocity in m/s, and the color scale is shown on the top of the figure. (right row) Latitudinal profiles of the vertical drift velocity as measured by the F15 (red), F16 (violet), and F17 (green) satellite. The UT of the beginning and the end of the satellite passes is indicated in the top and bottom of the figures. Thin gray lines show the standard deviations of the V_z flow calculated over 24 data points for F15 and over 6 points for F16.

estimate the ion sound velocity to be 1053 m/s and 1022 m/s for the two events, respectively (Table 1). Therefore, both our events are supersonic.

We note that the previous and the subsequent passes of the DMSP satellites did not show signatures of the fast plasma motion. Though the intensive irregularities continued to occur above the Pacific region until ~15 UT as shown by *Zakharenkova et al.* [2015], we do not observe fast plasma drift structures after ~11.7 UT. The detection of intensive irregularities around the area of the Eastern Pacific region during 5 h was proved by ground-based GPS-receivers, ionosondes, and by three Swarm satellites; however, unfortunately, no other instruments were available to verify the detection of the supersonic velocities around the region under consideration. The three Swarm satellites and the DMSP F18 satellite passed over the eastern Pacific region 2 h later, while the C/NOFS experienced a data transmission failure on 19 February 2014 (R. Heelis, private communication, 2015).

4. Discussions

The scientific literature does mention the detection of the supersonic and high-speed upward plasma drift; however, all those events seemed to be registered only in the postsunset sector [*Aggson et al.*, 1992; *Hysell et al.*, 1994; *Hanson et al.*, 1997]. To our knowledge, our observations are the first registration of the supersonic upward flow in the postmidnight-predawn sector. Both events occurred very close to the magnetic dip equator and at the early morning hours (~3–5 LT). The supersonic structures were detected at ~835–350 km of altitude (i.e., in the topside ionosphere), above the eastern Pacific region, separated by ~35° of longitude in space and by 45 min in time. The observed two events appeared to have different spatial structure: the first extended to about 385 km (3.5° of latitude) and could be attributed either to a wall of a “dead” plasma bubble or to a “simple” small plasma irregularity whereas the second extended up to ~1500 km and seemed to occur inside a plasma bubble. In addition, besides the two supersonic plasma drift structures, we have observed

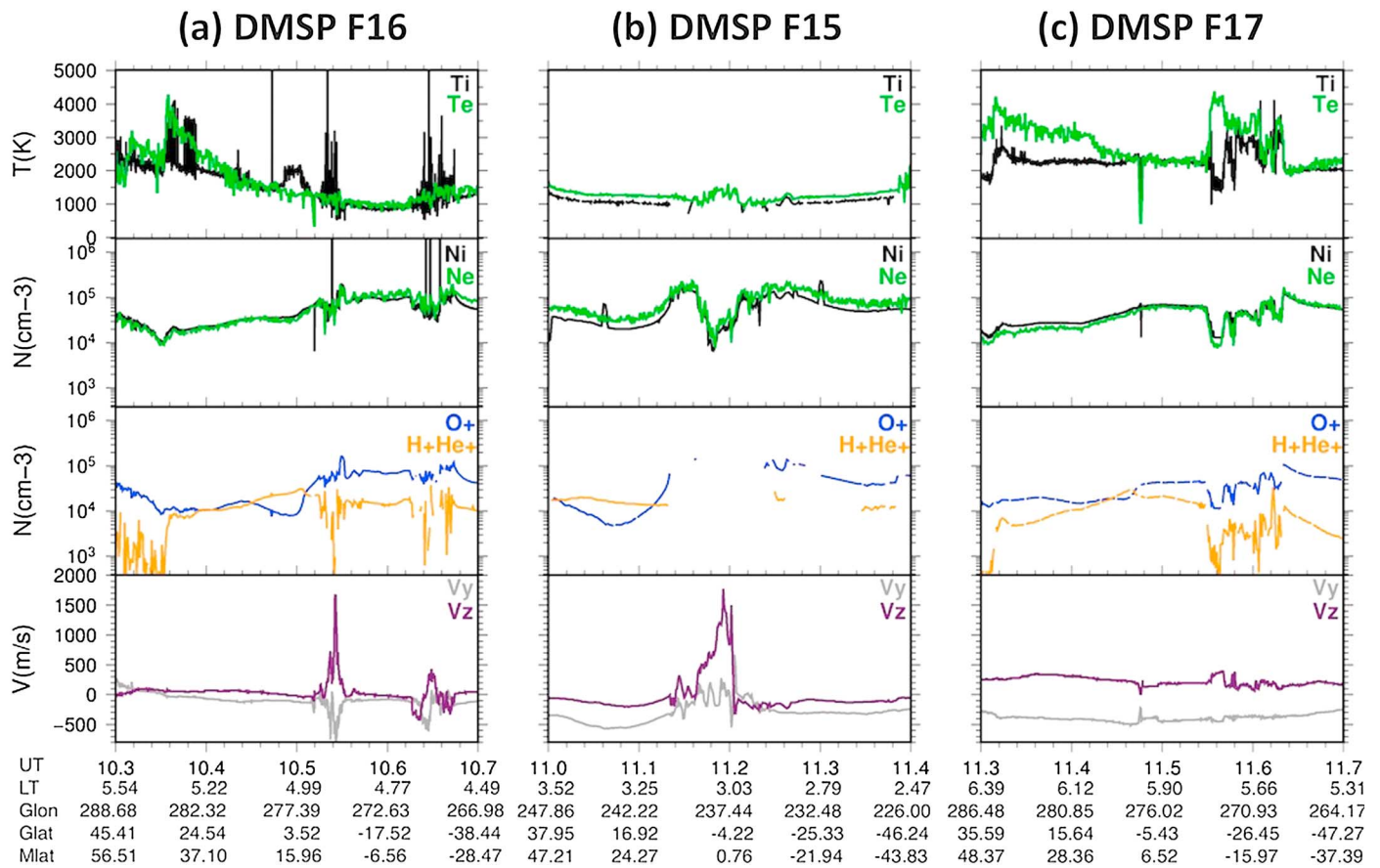


Figure 3. Parameters of the ionospheric plasma as measured by the (a) DMSP F15, (b) DMSP F16, and (c) DMSP F17 satellites while flying around the turbulence area. Figures 3a–3c (first row to fourth row) show the following: ion temperature (T_i , black) and electron temperature (T_e , green); ion density (N_i , black), and electron density (N_e , green); the oxygen density (O^+ , blue) and light ions (hydrogen H^+ and helium He^+ density (orange); vertical drift velocity (V_z , violet); and the DMSP cross-track (zonal) plasma drift velocity (V_y , gray). The UT, LT, GLAT, GLON, MLAT are shown below the figures.

another high-speed downward and upward flow structure with velocities up to ± 500 m/s. The latter area of intensive ionospheric irregularities persisted for at least 1 h, as shown by data from two DMSP satellites, while the plasma drift velocities decreased with time.

In the both supersonic cases, we observed simultaneous change in the horizontal plasma drift. The direction of the horizontal plasma motion was different from the ambient zonal motion, which is in agreement with observations by Huang *et al.* [2010] who mentioned that in the evening sector the zonal drift velocity of the plasma particles inside plasma bubbles can significantly contrast as compared to the ambient plasma drift velocity. Our observations show the same result for the predawn bubbles. One other interesting feature is the opposite zonal directions of the plasma flow inside the two detected supersonic structures: it is westward inside the first structure (detected by DMSP F16) and eastward inside the second event (detected by DMSP F15) (Figures 3a and 3b). Plasma bubbles are often reported to drift eastward in the premidnight sector and westward in the predawn sector, and the reverse of the drift direction occurs between the midnight [Taylor *et al.*, 1997] and around 4 UT [Abdu *et al.*, 1985; Fejer, 1991]. From our results, it follows that on 19 February the reverse of the equatorial plasma drift occurred between these two structures, i.e., between ~ 3 and ~ 5 LT.

Table 1. Main Plasma Characteristics at the Time and Place of the Two High-Speed Events Detection on 19 February 2014

	Location (GLon; GLat)	UT	LT/MLT	H (km)	DMSP	V_z -Max (m/s)	C_s (m/s)	Temperatures (K)	E_y (mV/m)
1	275.39; -5.42	10.54	4.79/4.8	854.7	F16	1638.2	1053	T_i -1652 T_e -1290	31
2	237.72; -2.80	11.19	3.04/2.91	835.3	F15	1770.6	1022	T_i ----- T_e -1220	---

Certainly, the main question here is on the source generating the observed high-speed plasma drift. It is known that the dominant role in the initiation of the growth of the R-T instability and the consequent generation of plasma irregularities is played by the zonal electric field that is responsible for the upward vertical drift. Following an initial spatial perturbation in the bottomside F region, the gravitationally induced current should cause a polarization electric field, provoking the depleted region to drift upward with respect to the surrounding plasma. An eastward directed background electric field (upward $E \times B$ drift) can also be enhanced in such a depleted region, thus assisting in its upward motion. While the gravitationally induced polarization field will always produce an upward drift of the depleted plasma region, the background electric field may be directed to the west (downward $E \times B$ drift) and hinder or even reverse such motion.

During geomagnetically quiet days, the “background” equatorial electric field is westward on the night side, whereas during geomagnetic disturbances it can reverse to eastward and serve as the source of the enhanced $E \times B$ drift on the nightside. The main mechanism perturbing the electric field over long time scales during geomagnetic storms is the dynamo electric fields caused by neutral winds [Blanc and Richmond, 1980], the prompt penetration electric fields, and the shielding/overshielding electric fields [Huang, 2008; Huang et al., 2013]. These storm time effects often have largest amplitude at ~ 04 LT [Fejer et al., 1991]. The prompt penetration electric fields occur during the IMF B_z negative turning and about 5–12% of the interplanetary electric field (IEF) can penetrate into the ionosphere [e.g., Kelley et al., 2003; Huang, 2008]. A sudden northward B_z turning from steady southward direction can also lead to anomalous reversal of the zonal equatorial electric fields [Kelley et al., 1979], and the penetration can be as efficient as during B_z negative events [Manoj et al., 2008].

It is also known that penetration of the IEF can take place even under low geomagnetic activity, but during short-time oscillations of the IMF B_z [Wei et al., 2008]. Under such conditions, during discontinuous magnetic reconnection associated with the multiple pulse-like reconnection electric field, short dawn-dusk IEF pulses can penetrate into ionosphere without shielding and affect the zonal electric field.

In our case study events, the supersonic upflows occurred at the beginning of the recovery phase of the geomagnetic storm of 19 February 2014. However, despite the fact that the $SYM-H$ index started to grow from ~ 09 UT, indicating the beginning of the recovery storm phase, at $\sim 09:30$ UT the IMF B_z turned southward for about 20–25 min (Figure 1a). From ~ 10.3 UT the IMF B_z was positive again until ~ 12 UT. Such fluctuations of the IMF B_z caused fluctuations and reversal of the interplanetary electric field (IEF) E_y component (Figure 1a, black curve) that is calculated as $-B_z * V_x$ from the solar wind velocity (V_x) and the IMF B_z (<http://omniweb.gsfc.nasa.gov>). Figure 1 demonstrates that both supersonic events occurred shortly after the second reverse of these parameters and when the IMF B_z was positive (i.e., northward), which presumes eastward electric field in the nighttime equatorial ionosphere [e.g., Huang et al., 2013]. We consider, therefore, that the increase of the equatorial electric field, due to the overshielding electric fields associated with a northward turning of the IMF B_z component led or at least contributed to the generation of the high-speed plasma drift in the early morning sector.

In addition to the storm time electric fields, the morning sector bubbles can result from traveling atmospheric and ionospheric disturbances (TADs and TIDs) that are generated at high-latitudes during substorms and further propagate equatorward. The TADs and TIDs can raise the height of the ionospheric F2 layer and, consequently, lead to development of the R-T instability [Bowman, 1978; Burke, 1979]. On our case, it is difficult to identify the passage of the TADs and TIDs above the turbulent area, because of no observational tools available over the ocean at that moment of time. We could see an increase of the O+ fraction during the supersonic event detection (Figure 3), which indicates the ionospheric uplift at least over the areas of observation of the two supersonic events.

The closest ionosonde station is located at Jicamarca Observatory (283.2°GLon ; -12.0°GLat), which is about 8 and 42° of longitude away from the two supersonic events, and, generally speaking, the ionospheric conditions at the events' place can differ from those above the digisonde. However, in absence of closer instruments, it is useful to analyze data from the Jicamarca digisonde (Figure 1c). One can see that at 10:00–11:30 UT there occurred sudden ± 40 m/s variations of the vertical ionospheric drifts, which corresponds to the time of the IMF B_z and the IEF E_y oscillations (Figure 1a). The latter signifies that the ionospheric vertical drift variations were, most likely, due to the prompt penetration of electric fields. These rapid short-term ionospheric vertical drift oscillations caused the F2 layer uplift and the F2 density enhancement over Jicamarca [Zakharenkova et al., 2015]. From Figure 1, we notice that the supersonic events occurred during the most rapid changes in the vertical drift.

To further analyze the situation within the regions of the supersonic events detection, we show results from the National Center for Atmospheric Research Thermosphere-Ionosphere-Electrodynamics General Circulation Model (TIE-GCM) [Roble *et al.*, 1988] simulation (Figure S2). One can see that the region #1 (the region of detection of the event #1, black triangle) experienced a convergence of neutral winds, as we see that at that location eastward and westward winds meet (Figures S2c and S2d), which might have contributed and accelerated the upward drifts. However, no particular features can be seen around the region #2 (violet triangle, Figures S2f–S2g).

Finally, concerning the DMSP detection of the supersonic upward plasma drifts, a very important question is on the data quality and the reliability of DMSP performance during these events detection. To check this issue, we first made sure that all the measurements performed in high-density plasma, i.e., the total ion density exceeded 10^3 ions/m³ (Figure 3). Second, it is known that the RPA and IDM instruments are designed to provide the best results in predominantly O⁺ plasma environment. When the percentage of light ions (H⁺ and He⁺) in the plasma increases above 15%, the IDM is compromised and the quality of the data degrades [e.g., Hairston and Heelis, 1996; Drayton *et al.*, 2005; <http://cindispace.utdallas.edu/DMSP/quality.htm>]. In the case of the 19 February 2014 events, the results are reliable, since the O⁺ density is sufficiently high (>90%) as compared to the light ions density (Figure 3). During the DMSP F15 detection, the O⁺ and light ions density were not measured; however, just around the event the O⁺ density is an order high than that of light ions (Figure 3b). In addition, in both cases, the standard deviations are below 206 m/s (thin gray lines in Figure 2, panels on the right), which also confirms the reliability of the detection.

5. Conclusions

By utilizing data from two DMSP satellites, we detected two very unusual cases of the upward plasma drifting at supersonic velocities in the local morning sector. Both high-speed events were observed above the eastern Pacific region, separated by $\sim 35^\circ$ of longitude in space and by 45 min in time. The events of ~ 1770 m/s and ~ 1683 m/s were detected at the recovery phase of the geomagnetic storm of 19 February 2014, during short-term oscillations of the IMF B_z and IEF E_y components. The latter is known to provoke the storm time penetration electric fields and to impact the equatorial electrodynamics, by reversing the background nighttime zonal electric field from westward to eastward and by triggering the R-T instability. We consider the storm time penetration electric fields to be the principal driver of the observed supersonic events, and neutral winds might have contributed and reinforced the unusual conditions.

Our case study event of 19 February 2014 seems to be a unique event, especially considering the quasi-simultaneous detection of two supersonic structures by several instruments around the same area, and our work, therefore, opens new horizons of the equatorial plasma bubbles behavior.

Acknowledgments

This work is supported by the European Research Council (ERC, grant agreement 307998). We acknowledge the NASA/GSFC's Space Physics Data Facility's OMNIWeb service for the data of interplanetary and geophysical parameters and the NGDC NOAA (<ftp://satdat.ngdc.noaa.gov/dmosp/>) and the University of Texas at Dallas for the DMSP data. We thank Robert Redmon (NOAA) and William Denig (NOAA) for their help with the DMSP data quality check at the first stage of this work. We are grateful to Marc Hairston and William Coley and to the Center for Space Sciences of the University of Texas at Dallas for their help with the additional data quality check. We thank Joseph Huba (NRL) for useful suggestions. The TIE-GCM simulation results have been provided by the Community Coordinated Modeling Center (CCMC) at GSFC through their public Runs on Request system (<http://ccmc.gsfc.nasa.gov>). The CCMC is a multiagency partnership between NASA, AFMC, AFOSR, AFRL, AFWA, NOAA, NSF, and ONR. The TIE-GCM Model was developed at the U.S. National Center for Atmospheric Research by Raymond G. Roble and collaborators.

References

- Abdu, M., I. Batista, J. Sobral, E. de Paula, and I. Kantor (1985), Equatorial ionospheric plasma bubble irregularity occurrence and zonal velocities under quiet and disturbed conditions, from polarimeter observations, *J. Geophys. Res.*, *90*(A10), 9921–9928, doi:10.1029/JA090iA10p09921.
- Aggson, T. L., W. J. Burke, N. C. Maynard, W. B. Hanson, P. C. Anderson, J. A. Slavin, W. R. Hoegy, and J. L. Saba (1992), Equatorial bubbles updrafting at supersonic speeds, *J. Geophys. Res.*, *97*(A6), 8581–8590, doi:10.1002/92JA00644.
- Astafyeva, E., Y. Yasukevich, A. Maksikov, and I. Zhivetiev (2014), Geomagnetic storms, super-storms and their impact on GPS-based navigation, *Space Weather*, *12*, 5085–5525, doi:10.1002/SW001072.
- Basu, S., S. Basu, J. J. Makela, E. MacKenzie, P. Doherty, J. W. Wright, F. Rich, M. J. Keskinen, R. E. Sheehan, and A. J. Coster (2008), Large magnetic storm-induced nighttime ionospheric flows at midlatitudes and their impacts on GPS-based navigation systems, *J. Geophys. Res.*, *113*, A00A06, doi:10.1029/2008JA013076.
- Blanc, M., and A. D. Richmond (1980), The ionospheric disturbance dynamo, *J. Geophys. Res.*, *85*, 1669–1686, doi:10.1029/JA085iA04p01669.
- Bowman, G. G. (1978), A relationship between polar magnetic substorms, ionospheric height rises and the occurrence of spread-F, *J. Atmos. Terr. Phys.*, *40*, 713–722.
- Burke, W. J. (1979), Plasma bubbles near the dawn terminator in the topside ionosphere, *Planet. Space Sci.*, *27*, 1187–1193.
- Burke, W. J., and T. L. Aggson (1993), A physical model for nonlinear, supersonic equatorial bubbles, *Nonlinear Process. Phys.*, 153–175.
- Burke, W. J., C. Y. Huang, C. E. Valladares, J. S. Machuzak, L. C. Gentile, and P. J. Sultan (2003), Multipoint observations of equatorial plasma bubbles, *J. Geophys. Res.*, *108*(A5), 1221, doi:10.1029/2002JA009382.
- Burke, W. J., O. de La Beaujardière, L. C. Gentile, D. E. Hunton, R. F. Pfaff, P. A. Roddy, Y.-J. Su, and G. R. Wilson (2009), C/NOFS observations of plasma density and electric field irregularities at post-midnight local times, *Geophys. Res. Lett.*, *36*, L00C09, doi:10.1029/2009GL038879.
- Dao, E., M. C. Kelley, P. Roddy, J. Retterer, J. O. Ballenthin, O. de La Beaujardiere, and Y.-J. Su (2011), Longitudinal and seasonal dependence of nighttime equatorial plasma density irregularities during solar minimum detected on the C/NOFS satellite, *Geophys. Res. Lett.*, *38*, L10104, doi:10.1029/2011GL047046.
- de la Beaujardière, O., J. M. Retterer, R. F. Pfaff, P. A. Roddy, C. Roth, W. J. Burke, and D. L. Cooke (2009), C/NOFS observations of deep plasma depletions at dawn, *Geophys. Res. Lett.*, *36*, L00C06, doi:10.1029/2009GL038884.

- Demyanov, V. V., Y. V. Yasukevich, A. B. Ishin, and E. I. Astafyeva (2012), Effects of ionosphere super-bubble on GPS performance depending on the bubble orientation relative to geomagnetic field, *GPS Solution*, *16*(N2), 181–189, doi:10.1007/s10291-011-0217-9.
- Drayton, R. A., A. V. Koustov, M. R. Hairston, and J.-P. Villain (2005), Comparison of DMSP cross-track ion drifts and SuperDARN line-of-sight velocities, *Ann. Geophys.*, *23*, 2479–2486.
- Fejer, B. G. (1991), Low latitude electrodynamic plasma drifts: A review, *J. Atmos. Terr. Phys.*, *53*(8), 677.
- Fejer, B. G., E. R. de Paula, S. Gonzalez, and R. F. Woodman (1991), Average vertical and zonal *F* region plasma drifts over Jicamarca, *J. Geophys. Res.*, *96*, 13,901–13,906, doi:10.1029/91JA01171.
- Fejer, B. G., L. Scherliess, and E. R. de Paula (1999), Effects of the vertical plasma drift velocity on the generation and evolution of equatorial spread *F*, *J. Geophys. Res.*, *104*(A9), 19,859–19,869, doi:10.1029/1999JA900271.
- Gentile, L. C., W. J. Burke, P. A. Roddy, J. M. Retterer, and R. T. Tsunoda (2011), Climatology of plasma density depletions observed by DMSP in the dawn sector, *J. Geophys. Res.*, *116*, A03321, doi:10.1029/2010JA016176.
- Hairston, M. R., and R. A. Heelis (1996), Analysis of ionospheric parameters based on DMSP SSIES data using the DBASE4 and NADIA programs, Tech. Rep., PL-TR-96-2078, Phillips Lab., Geophys. Dir., Hanscom Air Force Base, Mass.
- Hanson, W. B., W. R. Colet, R. A. Heelis, and A. L. Urquhart (1997), Fast equatorial bubbles, *J. Geophys. Res.*, *102*(A2), 2039–2045, doi:10.1029/96JA03376.
- Huang, C.-S. (2008), Continuous penetration of the interplanetary electric field to the equatorial ionosphere over eight hours during intense geomagnetic storms, *J. Geophys. Res.*, *113*, A11305, doi:10.1029/2008JA013588.
- Huang, C.-S., O. de La Beaujardière, R. F. Pfaff, J. M. Retterer, P. A. Roddy, D. E. Hunton, Y.-J. Su, S.-Y. Su, and F. J. Rich (2010) Zonal drift of plasma particles inside equatorial plasma bubbles and its relation to the zonal drift of the bubble structure. *J. Geophys. Res.*, *115*, A07316, doi:10.1029/2010JA015324.
- Huang, C.-S., O. de La Beaujardiere, P. A. Roddy, D. E. Hunton, J. O. Ballenthin, and M. R. Hairston (2013), Long-lasting daytime equatorial plasma bubbles observed by the C/NOFS satellite, *J. Geophys. Res. Space Physics*, *118*, 2398–2408, doi:10.1002/jgra.50252.
- Huba, J. D. (2013), NRL plasma formulary. [Available at http://www.nrl.navy.mil/ppd/sites/www.nrl.navy.mil/ppd/files/pdfs/NRL_FORMULARY_13.pdf].
- Huba, J. D., and G. Joyce (2007), Equatorial spread *F* modeling: Multiple bifurcated structures, secondary instabilities, large density 'bite-outs,' and supersonic flows, *Geophys. Res. Lett.*, *34*, L07105, doi:10.1029/2006GL028519.
- Hysell, D. L., M. C. Kelley, W. E. Swartz, and D. T. Farley (1994), VHF radar and rocket observations of equatorial spread-*F* on Kwajalein, *J. Geophys. Res.*, *99*(A8), 15,065–15,085, doi:10.1029/94JA00476.
- Kelley, M. C., B. G. Fejer, and C. A. Gonzales (1979), An explanation for anomalous equatorial ionospheric electric fields associated with a northward turning of the interplanetary magnetic field, *Geophys. Res. Lett.*, *6*(4), 301–304, doi:10.1029/GL006i004p00301.
- Kelley, M. C., J. J. Makela, J. L. Chau, and M. J. Nicholls (2003), Penetration of solar wind electric field into the magnetosphere/ionosphere system, *Geophys. Res. Lett.*, *30*(4), 1158, doi:10.1029/2002GL016321.
- Kelly, M. A., J. M. Comberiate, E. S. Miller, and L. J. Paxton (2014), Progress toward forecasting of space weather effects on UHF SATCOM after Operation Anaconda, *Space Weather*, *12*, 601–611, doi:10.1002/2014SW001081.
- Li, J., G. Ma, T. Maruyama, and Z. Liu (2012), Mid-latitude ionospheric irregularities persisting into late morning during the magnetic storm on 19 March 2001, *J. Geophys. Res.*, *117*, A08304, doi:10.1029/2012JA017626.
- Manoj, C., S. Maus, H. Luhr, and P. Alken (2008), Penetration characteristics of the interplanetary electric field to the daytime equatorial ionosphere, *J. Geophys. Res.*, *113*, A12310, doi:10.1029/2008JA013381.
- McClure, W. H., W. Hanson, and J. Hoffman (1977), Plasma bubbles and irregularities in the equatorial ionosphere, *J. Geophys. Res.*, *82*(19), 2650–2656, doi:10.1029/JA082i019p02650.
- Ott, E. (1978), Theory of Rayleigh-Taylor bubbles in the equatorial ionosphere, *J. Geophys. Res.*, *83*(A5), 2066–2070, doi:10.1029/JA083iA05p02066.
- Patra, A. K., D. Tiwari, S. Sripathi, P. B. Rao, R. Sridharan, C. V. Devasia, K. S. Viswanathan, K. S. V. Subbarao, R. Sekar, and E. A. Kherani (2005), Simultaneous radar observations of meter-scale *F* region irregularities at and off the magnetic equator over India, *J. Geophys. Res.*, *110*, A02307, doi:10.1029/2004JA010565.
- Roble, R. G., E. C. Ridley, A. D. Richmond, and R. E. Dickinson (1988), A coupled thermosphere/ionosphere general circulation model, *Geophys. Res. Lett.*, *15*(12), 1325–1328, doi:10.1029/GL015i012p01325.
- Taylor, M. J., J. V. Eccles, J. LaBelle, and J. H. A. Sobral (1997), High-resolution OI (630 nm) image measurements of *F*-region depletion drifts during the Guara Campaign, *Geophys. Res. Lett.*, *24*(13), 1699–1702, doi:10.1029/97GL01207.
- Wei, Y., M. Hong, W. Wan, A. Du, J. Lei, B. Zhao, W. Wang, Z. Ren, and X. Yue (2008), Unusually long lasting multiple penetration of interplanetary electric field to equatorial ionosphere under oscillating IMF Bz, *Geophys. Res. Lett.*, *35*, L02102, doi:10.1029/2007GL032305.
- Woodman, R. F., and C. La Hoz (1976), Radar observations of *F* region equatorial irregularities, *J. Geophys. Res.*, *81*, 5447–5466, doi:10.1029/JA081i031p05447.
- Yeh, H. C., S.-Y. Su, and R. A. Heelis (2001), Storm time plasma irregularities in the Pre-dawn hours observed by the low-latitude ROCSAT-1 satellite at 600 km, *Geophys. Res. Lett.*, *28*(4), 685–688, doi:10.1029/2000GL012183.
- Yizengaw, E., J. Retterer, E. E. Pacheco, P. Roddy, K. Groves, R. Caton, and P. Baki (2013), Postmidnight bubbles and scintillations in the quiet-time June solstice, *Geophys. Res. Lett.*, *40*, 5592–5597, doi:10.1002/2013GL058307.
- Yokoyama, T., M. Yamamoto, Y. Otsuka, M. Nishioka, T. Tsugawa, S. Watanabe, and R. F. Pfaff (2011), On postmidnight low-latitude ionospheric irregularities during solar minimum: 1. Equatorial atmosphere radar and GPS-TEC observations in Indonesia, *J. Geophys. Res.*, *116*, A11325, doi:10.1029/2011JA016797.
- Zakharenkova, I. E., and E. Astafyeva (2015), Topside ionospheric irregularities as seen from multi-satellite observations, *J. Geophys. Res. Space Physics*, *120*, 807–824, doi:10.1002/2014JA020330.
- Zakharenkova, I., E. Astafyeva, and I. Cherniak (2015), Early morning irregularities detected with space-borne GPS measurements in the topside ionosphere: A multi-satellite case study, *J. Geophys. Res. Space Physics*, *120*, doi:10.1002/2015JA021447.